WILLIAM & MARY
CHARTERED 1693

W&M ScholarWorks

Undergraduate Honors Theses

Theses, Dissertations, & Master Projects

5-2010

The Dynamical Behavior of a Two Patch Predator-Prey Model

Yuanyun Liu
College of William and Mary

Follow this and additional works at: https://scholarworks.wm.edu/honorstheses

Recommended Citation

The Dynamical Behavior of a Two Patch Predator-Prey Model

A thesis submitted in partial fulfillment of the requirement
for the degree of Bachelors of Science in Mathematics from
The College of William and Mary

by

Yuanyuan Liu

Accepted for _____

_____
Junping Shi, Director

_____
Olivier Coibion

_____
Lawrence Leemis

_____
Jianjun Paul Tian

Williamsburg, VA
April 23, 2010

The Dynamical Behavior of
a Two Patch Predator-Prey Model

Yuanyuan Liu

Department of Mathematics,

College of William and Mary,

Williamsburg, VA 23187, USA

Email: yliu02@email.wm.edu

April 23, 2010

Abstract

A two-patch Rosenzweig-MacArthur system describing predator-prey interaction in a spatially inhomogeneous environment is investigated. The global stability of equilibrium solutions for the homogeneous case is proved using Lyapunov functional, and stability analysis for the coexistence equilibrium is also given. Numerical bifurcation diagrams and numerical simulations of the limit cycle dynamics for the inhomogeneous case are obtained to compliment theoretical approach. Some of our results help to explain and clarify possible solutions to the Paradox of Enrichment in ecological studies.

Contents

List of Figures

Chapter 1

Introduction

1.1 Background

In ecology, predation describes a biological interaction where a predator feeds on its prey. It takes on various forms in nature. Predators might or might not kill their prey prior to feed on them, but the act of predation always results to benefit of the predator. We can recognize a population of "predators" that benefits from feeding, and a population of "victims" that suffers. The key characteristic of predation, however, is the predator's direct impact on the prey population. A predator-prey model gives insight into the dynamics of predation through studying the population changes of predator and prey. Predation can also be described as a competitive interaction in nature that is mediated through populations of resources [7]; thus predation is called a "consumer-resource interaction" in a more general sense. In [24], the authors stated that the consumer-resource interaction is arguably the fundamental building block of ecological communities. Virtually every species is part of a consumer resource interaction, as a consumer of living resources, or as a resource for another species. If we are to understand population regulation and its various manifestations, we need to focus on consumer-resource interactions.

The equations describing predator-prey interaction were first derived independently

by Alfred J. Lotka in 1925 [18, 19] and Vito Volterra in 1926 [31]. Volterra's interest in the subject stemmed from his daughter's fiance, Humberto D'Ancona, a fisheries biologist who was trying to explain the observed increase in predator fish (and corresponding decrease in prey fish) in the Adriatic Sea during World War I. At the same time in the United States, the equations studied by Volterra were derived independently by Alfred Lotka to describe a hypothetical chemical reaction in which the chemical concentrations oscillate. The Lotka–Volterra model is based on linear per capita growth rates, which can be written as

$$\begin{cases} \dfrac{dN}{dt} = aN - bNP, \\ \dfrac{dP}{dt} = cNP - dP, \end{cases} \tag{1.1}$$

where N and P are the population densities of prey and predator, respectively; a and d are their per-capita rates of change in the absence of each other; and b and c are their rates of change due to interaction. Since the 1930s, modifications have been made on the original Lotka–Volterra equations. To correct the unreasonable assumption that the prey population grows infinitely in the absence of predators, a logistic self-limitation term is often added to the prey equation (see Pearl [25]):

$$\frac{dN}{dt} = aN \left(1 - \frac{N}{K} \right) - bNP. \tag{1.2}$$

Later, a logistic predator equation was considered by Leslie [21]:

$$\frac{dP}{dt} = cP \left(1 - e\frac{P}{N} \right), \tag{1.3}$$

where $1/e$ is the marginal reproductive value of the resource, and N/e is the carrying capacity of predators when provided with constant supply of prey. This modification makes the predator isocline slanting rather than vertical, which solves the paradox of enrichment and biological control, as stated by Berryman in [1].

One of the other unrealistic assumptions of the Lotka–Volterra model is that the predator can always increase their prey consumption as the prey population increases. The assumption of linear functional response [30], that the feeding rate per predator as a linear

function of prey abundance, later refereed as a *Holling Type I* functional response was unrealistic because there is a limit to the rate at which individual predator can consume prey. Thus, the term feeding rate n/t, the rate at which individual predator captures prey was introduced and new types of predator functional response were constructed. Holling [9] derived his famous "disk" function which is identical to the Michaelis–Menten equation of enzyme kinetics [27]:

$$\frac{n}{t} = \frac{mN}{w + N},$$ (1.4)

where m is the maximum and constant rate of prey consumption per predator, and w is the prey density where the attack rate is half-saturated. This is also called *Holling Type II* functional response. Finally, a *Holling Type III* functional response can be described as

$$\frac{n}{t} = \frac{mN^2}{w^2 + N^2},$$ (1.5)

where the feeding rate is accelerated at low prey density, but decreases at high prey density as the asymptote is reached. Figure 1.1 shows the graph of all three types of functional responses.
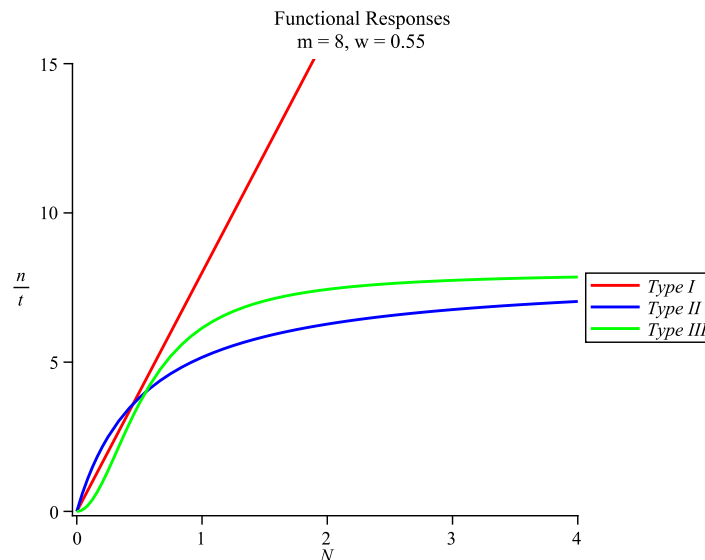

Figure 1.1: Three Types of Holling Functional Responses

The functional responses have important consequences for the ability of predators to control victim populations. Figure 1.2 shows the proportion of the prey population that is consumed by an individual predator as prey abundance increase.

Proportion of the prey population that is consumed
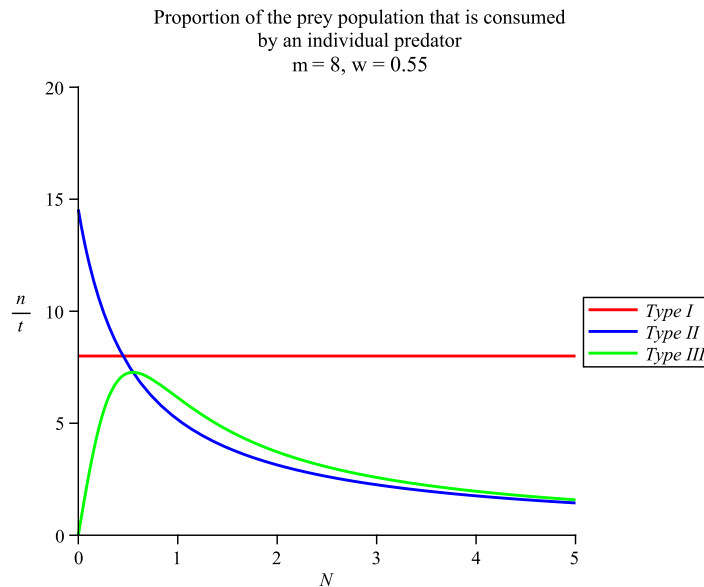by an individual predator
m = 8, w = 0.55

Figure 1.2: Prey Population Control Under Different Types of Functional Responses

For the *Type I* response of the simple Lotka-Volterra model, this proportion of predator and prey remains a constant, because each predator increases its individual feeding as prey abundance increases. For the *Type II response*, the proportion decrease steadily because each predator can only process prey at a maximum rate k. The *Type III* response shows an initial increase because of the accelerated feeding rate, but this quickly decreases and converges on the *Type II* curve. These curves show that, at a high prey abundance, predators with a *Type II* and *Type III* response may not be able to effectively control prey populations.

A later version of predator-prey model was developed by Rosenzweig and MacArthur [28] has a logistic growth rate and a *Holling type II* functional response. Their equations

4

(in modern notation) are

$$\frac{dU}{ds} = \gamma U\left(1 - \frac{U}{K}\right) - \frac{CMUV}{A+U}, \quad \frac{dV}{ds} = -DV + \frac{MUV}{A+U}, \qquad (1.6)$$

where the number of prey U satisfies a logistic growth pattern; $\gamma > 0$ represents the intrinsic growth rate of the prey; $K > 0$ is the carrying capacity of the prey; $D > 0$ is the death rate of the predator; $C > 0$ measures the relative loss of the prey; the functional response of the predator, which corresponds to saturation of their appetites and reproductive capacity, is of Holling type II in form $MU/(A+U)$ here. The Rosenzweig–MacArthur model (1.6) is considered to be a realistic predator-prey model [7, 23, 24]. In many recent investigations, it has been used as prototypical predator-prey model as the base of more advanced models [5, 6, 8].

For a class of conventional predator-prey interaction models including Rosenzweig-MacArthur model (1.6), it is known that a stable limit cycle exists for a range of parameters. Extensive studies [14, 32] have shown that equilibrium solutions and periodic solutions dominate the asymptotic behavior of the system. Mathematical theory has been established [12, 13] to show that, for certain parameters, the prey-only equilibrium or coexistence equilibrium is globally stable; and for other parameters, a periodic orbit attracts all solutions [2, 15]. In 1971, Rosenzweig showed in [26] that increasing the supply of limiting nutrients or energy tends to destroy the steady state, which is known as "Paradox of Enrichment".

The two-patch model in this thesis is based on Rosenzweig-MacArthur model, and a detailed analysis of Rosenzweig-MacArthur model (1.6) will be reviewed in Section 2.1.

1.2 Spatial Predator-Prey Models

The natural environment for most biological species is heterogeneous in space. Therefore it is reasonable to expect the dynamics of their populations to be influenced by the heterogeneity of the environment, apart from the interactions between the species. This

query has inspired studies focused on equilibriums of predator-prey system with diffusion. As early as 1979, de Mottoni and Rothe [4] generalized the Volterra–Lotka system with diffusion, and they obtained asymptotic stability of homogeneous equilibrium states. Another paper by Holt [10] in 1984 studied the impact of spatial heterogeneity and indirect interactions on the coexistence of prey species.

Similar questions concerning coupled chemical reactors have also been raised and widely studied in chemistry. Lengyel and Epstein [20] analyzed conditions for stable homogeneous steady state to lose stability as a result of coupling, and they found that diffusion-induced instability can lead to multiple stable steady states, oscillatory states and even chaos. The model of the Chlorine Dioxide-Iodine Malonic Acid (CDIMA) reaction that Lengyel and Epstein built in 1990 has also inspired other researchers to work on Turing instability in diffusively coupled chemical model [11, 29].

More recent biological studies have yielded various results. Commins and Hassell [3] extended the question of spatial interactions to wider question of community structure by considering various three-species systems, and they found multi-species coexistence can occur despite unstable local populations. Jansen argued in [17] that spatial predator-prey populations can be regulated through the interplay of local dynamics and migration. Furthermore, he suggested in [16] that this regulation through spatial interactions can be a possible solution to the Paradox of Enrichment. In more recent studies, Goldwyn and Hastings stated in [5, 6] that small heterogeneity has large effects on synchronizing populations. Holland and Hastings [8] showed a contrasting result that randomizing the structure of dispersal networks tends to favor asynchrony and prolonged transient dynamics.

1.3   Summary of Results

This paper investigates the global dynamical behavior of a spatially heterogenous biological system with two patches. The system describes a predator-prey interaction and

the dispersal between two spatial patches. We use both analytic techniques such as Lyapunov functions, linearization and bifurcation theory, as well as numerical approach using `Matlab`. In Chapter 2, we prove the global stability of equilibrium solution with Lyapunov functional technique, and we also use the linearization method and linear algebra to consider the stability of equilibrium solutions. Numerical bifurcation diagrams of equilibria and limit cycles motivated by these theoretical studies are obtained with `Matlab` function `MatCont`. In Chapter 3, we consider spatially non-homogenous systems, and we study the impact of the spatial heterogeneity to the global dynamics.

Chapter 2

Mathematical Analysis of Symmetric Model

2.1 Analysis of Rosenzweig-MacArthur Model

The original Rosenzweig-MacArthur predator-prey model is as (1.6), and it has been thoroughly studied in existing papers. We review this well-known dynamics, and we mostly follow [14]. A series of change of variables is carried out to simplify the equations:

$$t = \gamma \cdot s, \quad u = \frac{U}{K}, \quad \text{and} \quad v = \frac{C}{K} \cdot V,$$

then the dimensionless system of equations

$$\begin{cases} u' = u\left(1 - \dfrac{u}{K}\right) - \dfrac{muv}{1+u}, \\ v' = \dfrac{muv}{1+u} - ev, \end{cases} \tag{2.1}$$

is obtained where

$$m = \frac{M}{\gamma}, \quad d = \frac{D}{\gamma}, \quad \text{and} \quad a = \frac{A}{K}.$$

Equation (2.1) is the local predator-prey system in each patch for our model.

The predator-prey system (2.1) has three steady state solutions: $(0,0)$, $(K,0)$, (λ, v_λ), where $\lambda = \dfrac{e}{m-e}$ and $v_\lambda = \dfrac{(K-\lambda)(1+\lambda)}{mK}$. The coexistence equilibrium (λ, v_λ) is in the

first quadrant if and only if $e < \dfrac{mK}{K+1}$ (or $0 < \lambda < K$). When $e \geq \dfrac{mK}{K+1}$ (or $\lambda \geq K$), $(K, 0)$ is globally asymptotically stable. Hence we always assume that $0 < e < \dfrac{mK}{K+1}$ in the following.

The global stability of (λ, v_λ) can be established through a Lyapunov function (see [12, 13]):

$$W(u, v) = \int_\lambda^u \frac{p(\xi) - e}{p(\xi)} d\xi + \int_{v_\lambda}^v \frac{\eta - v_\lambda}{\eta} d\eta, \tag{2.2}$$

where $p(u) = \dfrac{mu}{1+u}$. From straightforward calculation,

$$\dot{W}(u(t), v(t)) = [p(u) - p(\lambda)] \cdot [v_0(u) - v_0(\lambda)], \tag{2.3}$$

where

$$v_0(u) = \frac{u(1 - u/K)}{p(u)} = \frac{(1+u)(K-u)}{mK}. \tag{2.4}$$

If $K \leq 1$, then $v_0'(u) < 0$ for any $u > 0$. Hence when $K \leq 1$, $\dot{W} < 0$ along an orbit $(u(t), v(t))$ of (2.1) and $\dot{W} = 0$ only if $(u(t), v(t)) = (\lambda, v_\lambda)$. Thus (λ, v_λ) is globally asymptotically stable when $K \leq 1$. On the other hand, if $K > 1$, but $v_\lambda \leq 1/m$ (which is equivalent to $v_0(\lambda) \leq v_0(0)$), then $[p(u) - p(\lambda)] \cdot [v_0(u) - v_0(\lambda)] \leq 0$ for any $u > 0$, and (λ, v_λ) is also globally asymptotically stable in this case. We notice that $v_\lambda \leq 1/m$ is equivalent to

$$\lambda \geq K - 1. \tag{2.5}$$

That leaves the case: for any $K, m > 0$,

$$K > 1, \quad \text{and} \quad 0 < e < \frac{m(K-1)}{K} \quad \text{(or equivalently } 0 < \lambda < K - 1). \tag{2.6}$$

The dynamics of (2.1) under (2.6) is completely understood. The local stability of (λ, v_λ) can be determined from the linearization at the equilibrium. We use λ as the bifurcation parameter. The Jacobian at (λ, v_λ) is

$$J = \begin{pmatrix} \dfrac{\lambda(K - 1 - 2\lambda)}{(1+\lambda)K} & -\dfrac{m\lambda}{1+\lambda} \\ \dfrac{K - \lambda}{K(1+\lambda)} & 0 \end{pmatrix}. \tag{2.7}$$

10

Then $\lambda_* = \dfrac{K-1}{2}$ is a Hopf bifurcation point. When $\dfrac{K-1}{2} < \lambda < K$, (λ, v_λ) is locally asymptotically stable. Indeed the local stability implies the global asymptotical stability of (λ, v_λ) from the Poincaré–Bendixon theory. Finally when $0 < \lambda < \dfrac{K-1}{2}$, (λ, v_λ) is locally unstable, and (2.1) possesses a unique limit cycle which is globally asymptotically orbital stable (see [2, 15]).
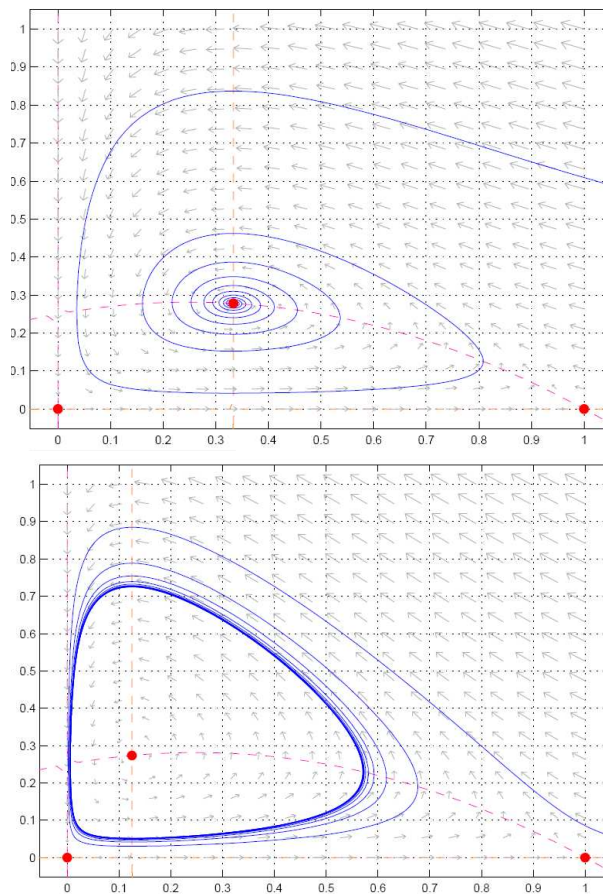

Figure 2.1: Phase portraits of (2.1). (upper) $\dfrac{K-1}{2} < \lambda < K$, (λ, v_λ) is globally asymptotically stable; (lower) $0 < \lambda < \dfrac{K-1}{2}$, the unique limit cycle is globally asymptotically orbital stable.

In summary, there are three possible asymptotic dynamic behaviors for the predator-prey model (2.1):

1. When $\lambda \geq K$, the equilibrium $(K, 0)$ is globally asymptotically stable (predator extinction);

2. When $K > 1$ and $\dfrac{K-1}{2} < \lambda < K$, or $K \leq 1$ and $0 < \lambda < K$, the coexistence equilibrium (λ, v_λ) is globally asymptotically stable (coexistence);

3. When $K > 1$ and $0 < \lambda < \dfrac{K-1}{2}$, a limit cycle is globally asymptotically stable (oscillatory).

If the parameters m and e are fixed, and we use the carrying capacity K as a bifurcation parameter, then

1. When $0 < K \leq \dfrac{e}{m-e}$, the equilibrium $(K, 0)$ is globally asymptotically stable (predator extinction);

2. When $\dfrac{e}{m-e} < K < \dfrac{m+e}{m-e}$, the coexistence equilibrium (λ, v_λ) is globally asymptotically stable (coexistence);

3. When $K > \dfrac{m+e}{m-e}$, a limit cycle is globally asymptotically stable (oscillatory).

The latter sequence of bifurcations when the carrying capacity increases is called paradox of enrichment [26]: the better environment destabilizes the coexistence of predator and prey; the oscillation puts the population density of either species very low for an extended period, which makes the population more vulnerable to the stochastic fluctuation.

2.2 Two-Patch Model

In this paper, we study a two-patch model for a Rosenzweig-MacArthur system, which is one of most widely used predator-prey models for ecological studies (see [7, 8, 12, 14, 22, 24, 26, 28]). This yields a system of four coupled ordinary differential equations. Within each patch, the prey population follows logistic growth, and the predation has a *Holling Type II* ([9]) functional response of predator to prey density. The two patches are coupled

through migration of both prey and predator. We assume the same migration rates over patches for prey and predator, respectively. The system of the equations takes the form:

$$
\begin{cases}
u' = f_1(u, v) + a(w - u), \\
v' = g_1(u, v) + c(x - v), \\
w' = f_2(w, x) - a(w - u), \\
x' = g_2(w, x) - c(x - v),
\end{cases}
\tag{2.8}
$$

where, for $i = 1, 2$,

$$
f_i(u, v) = u\left(1 - \frac{u}{K_i}\right) - \frac{m_i u v}{1 + u}, \quad g_i(u, v) = \frac{m_i u v}{1 + u} - e_i v.
\tag{2.9}
$$

The variables u and w denote the densities of the prey populations in each patch, while v and x denote the densities of the predator populations. The variables in (2.8) has been nondimensionalized to reduce the number of parameters. The parameters have the following interpretation: K_i, carrying capacity of the prey population; m_i, the saturation value of the functional response; e_i, the predator death rete in the absence of prey; a and c, the per capita prey migration rate and predator migration rate, respectively. If $K_1 = K_2$, $m_1 = m_2$ and $e_1 = e_2$, then the two patches are spatially homogeneous (symmetric); otherwise they are heterogeneous (nonsymmetric).

We comment that similar models have been used in several previous studies. In [16, 17], (2.8) was considered, but with immobile prey species $(a = 0)$; in [20], a system of form (2.8) was considered but with the kinetic model being the CDIMA chemical reaction not ecological ones. Numerical approaches were used in both papers. In [8], a coupled system with 10 patches with Rosenzweig-MacArthur predator-prey model was considered, and it is assumed the whole system is homogeneous with identical local dynamics.

13

2.3 Stability with Lyapunov Functional

For the two-patch model (2.8), we first consider the homogeneous patch case, that is: all parameters (K, m, e) are same for the two patches. The model then describes a homogenous environment where the effect of migration cancels out. The model is also symmetrical in the sense that we can construct the solution of (2.8) based on known solutions of (2.9).

Thus we want to know whether the symmetric equilibrium points $(K, 0, K, 0)$ and $(\lambda, v_\lambda, \lambda, v_\lambda)$ are globally stable for the symmetrical model of (2.8). To prove global stability, we will follow the methods introduced in [13] and construct Lyapunov functions. Define $p(u) = \dfrac{mu}{1+u}$ and $v(u) = \dfrac{(K-u)(1+u)}{mK}$. Then (2.8) is equivalent to

$$
\begin{cases}
u' = p(u)(v(u) - v) + a(w - u), \\
v' = v(p(u) - e) + c(x - v), \\
w' = p(w)(v(w) - x) - a(w - u), \\
x' = x(p(w) - e) - c(x - v).
\end{cases}
\tag{2.10}
$$

When $\lambda \geq K$, construct Lyapunov functions

$$
V_1(u, v) = \int_K^u \frac{p(\xi) - p(K)}{p(\xi)} \, d\xi + v
\tag{2.11}
$$

and

$$
V_2(w, x) = \int_K^w \frac{p(\xi) - p(K)}{p(\xi)} \, d\xi + x.
\tag{2.12}
$$

Then taking derivatives with respect to time t, we get

$$
\begin{aligned}
\frac{d}{dt} V_1(u(t), v(t)) &= \frac{p(u) - p(K)}{p(u)} \frac{du}{dt} + \frac{dv}{dt} \\
&= (p(u) - p(K))(v(u) - v) + v(p(u) - e) \\
&\quad + \frac{p(u) - p(K)}{p(u)} a(w - u) + c(x - v)
\end{aligned}
$$

14

and

$$\frac{d}{dt}V_2(w(t), x(t)) = \frac{p(w) - p(K)}{p(w)}\frac{dw}{dt} + \frac{dx}{dt}$$

$$= (p(w) - p(K))(v(w) - x) + x(p(w) - e)$$

$$- \frac{p(w) - p(K)}{p(w)}a(w - u) - c(x - v).$$

We construct a Lyapunov function for the two-patch model from (2.11) and (2.12), and we get

$$\frac{d}{dt}V_1(u(t), v(t)) + \frac{d}{dt}V_2(w(t), x(t)) =$$

$$(p(u) - p(K))v(u) + v(p(K) - p(\lambda))$$

$$+ (p(w) - p(K))v(w) + x(p(K) - p(\lambda)) + ae(w - u)\left(\frac{1}{p(w)} - \frac{1}{p(u)}\right).$$

When $\lambda \geq K$, $(p(u) - p(K))v(u) \leq 0$ for all $u \geq 0$; similarly, $(p(w) - p(K))v(w) \leq 0$ for all $w \geq 0$. Notice that p is an increasing function, then $(p(K) - p(\lambda))v \leq 0$ for all $v \geq 0$ and $(p(w) - p(K))v(w) \leq 0$ for all $x \geq 0$. Finally the last term $a(w - u)p(k)\left(\frac{1}{p(w)} - \frac{1}{p(u)}\right) \leq 0$ because p is increasing. V_1 and V_2 are Lyapunov functions in this case, and it follows from Theorem 3.2 in [12] that $(K, 0, K, 0)$ is globally stable.

Now we consider the case when $K - 1 < \lambda < K$. The equilibrium solution considered here is $(\lambda, v_\lambda, \lambda, v_\lambda)$, where $u_* = \lambda = \frac{e}{m - e}$ and $v_* = v_\lambda = \frac{(u + 1)(K - u)}{mK}$.
We define Lyapunov functions

$$V_3(u, v) = \int_{u_*}^{u} \frac{p(\xi) - p(u_*)}{p(\xi)}d\xi + \int_{v_*}^{v} \frac{\eta - v_*}{\eta}d\eta \qquad (2.13)$$

and

$$V_4(w, x) = \int_{w_*}^{w} \frac{p(\xi) - p(w_*)}{p(\xi)}d\xi + \int_{x_*}^{x} \frac{\eta - x_*}{\eta}d\eta. \qquad (2.14)$$

Thus,

$$\frac{d}{dt}V_3(u(t), v(t)) = \frac{p(u) - p(u_*)}{p(u)}\frac{du}{dt} + \frac{v - v_*}{v}\frac{dv}{dt}$$

$$= (p(u) - e)(v(u) - v_*) + a(w - u)\frac{p(u) - e}{p(u)} + c(x - v)\frac{v - v_*}{v}$$

15

and

$$\frac{d}{dt}V_4(w(t), x(t)) = \frac{p(w) - p(w_*)}{p(w)}\frac{dw}{dt} + \frac{x - x_*}{x}\frac{dx}{dt}$$

$$= (p(w) - e)(v(w) - w_*) - a(w - u)\frac{p(w) - e}{p(w)} - c(x - v)\frac{x - x_*}{x}.$$

Now we have

$$\frac{d}{dt}V_3(u(t), v(t)) + \frac{d}{dt}V_4(w(t), x(t))$$

$$=(p(u) - p(\lambda))(v(u) - v_\lambda) + (p(w) - p(\lambda))(v(w) - v_\lambda)$$

$$+ ae(w - u)\left(\frac{1}{p(w)} - \frac{1}{p(u)}\right) + cv_\lambda(x - v)\left(\frac{1}{x} - \frac{1}{v}\right).$$

When $K - 1 < \lambda < K$, $p(u)$ is increasing while $v(u)$ is decreasing, which makes the first two terms both less than or equal to 0. The last two terms are also less than or equal to 0. Then we know $\frac{d}{dt}V_3(u(t), v(t)) + \frac{d}{dt}V_4(w(t), x(t)) \leq 0$. We can again apply Theorem 3.2 in [12] to show that $(\lambda, v_\lambda, \lambda, v_\lambda)$ is a globally stable equilibrium.

We summarize the results in this section in the following theorem:

Theorem 2.1. *For the system of differential equations* (2.10), *if* $\lambda \geq K$, *then the equilibrium* $(K, 0, K, 0)$ *is globally asymptotically stable; if* $K - 1 < \lambda < K$, *then the equilibrium* $(\lambda, v_\lambda, \lambda, v_\lambda)$ *is globally asymptotically stable.*

2.4   Linear stability and instability

In an effort to examine the local stability of the two-patch model, we now consider a more general symmetric system:

$$\begin{cases} u' = f(u, v) + a(w - u), \\ v' = g(u, v) + c(x - v), \\ w' = f(w, x) - a(w - u), \\ x' = g(w, x) - c(x - v), \end{cases} \tag{2.15}$$

16

where

$$f(u,v) = u\left(1 - \frac{u}{K}\right) - \frac{muv}{1+u}, \quad g(u,v) = \frac{muv}{1+u} - ev, \tag{2.16}$$

or any two variable functions f and g modeling the interaction. We then apply a transformation similar to what Lengyel and Epstein used in [20] on population variables (u, v, w, x) by taking sums and differences. Let

$$\begin{cases} U = u + w, \\ V = v + x, \\ W = u - w, \\ X = v - x, \end{cases} \tag{2.17}$$

where U and V denote the sums of prey and predator population in the two patches, respectively, and W and X are the differences of the population. This transformation leads to a new system describing the dynamics of population sums and differences, this new parametrization can be expressed by the following set of equations:

$$\begin{cases} U' = f\left(\frac{U+W}{2}, \frac{V+X}{2}\right) + f\left(\frac{U-W}{2}, \frac{V-X}{2}\right), \\ V' = g\left(\frac{U+W}{2}, \frac{V+X}{2}\right) + g\left(\frac{U-W}{2}, \frac{V-X}{2}\right), \\ W' = f\left(\frac{U+W}{2}, \frac{V+X}{2}\right) - f\left(\frac{U-W}{2}, \frac{V-X}{2}\right) - 2aW, \\ X' = g\left(\frac{U+W}{2}, \frac{V+X}{2}\right) - g\left(\frac{U-W}{2}, \frac{V-X}{2}\right) - 2cX. \end{cases} \tag{2.18}$$

Based on the symmetry of the system and previous analysis in Section 2.1, local stability can be confirmed with the steady states $(0, 0, 0, 0)$ and $(2K, 0, 0, 0)$. We are interested in the local stability of the new coexistence equilibrium $(U, V, W, X) = (2\lambda, 2v_\lambda, 0, 0)$ of (2.18), where $\lambda = \frac{e}{m-e}$ and $v_\lambda = \frac{(K-\lambda)(1+\lambda)}{mK}$. The local stability of (λ, v_λ) with respect to (2.1) has been determined from the linearization at the equilibrium in Section 2.1, where we use λ as the bifurcation parameter. Here we use that information to consider the stability of $(2\lambda, 2v_\lambda, 0, 0)$ with respect to (2.18). The Jacobian at $(2\lambda, 2v_\lambda, 0, 0)$ is a

17

block matrix that can be described as

$$
J = \begin{pmatrix} M_1 & 0 \\ 0 & M_2 \end{pmatrix} = \begin{pmatrix} a_{11} & a_{12} & 0 & 0 \\ a_{21} & a_{22} & 0 & 0 \\ 0 & 0 & a_{11} - 2a & a_{12} \\ 0 & 0 & a_{21} & a_{22} - 2c \end{pmatrix}
\tag{2.19}
$$

where we notice that

$$
M_1 = \begin{pmatrix} \dfrac{\lambda(K - 1 - 2\lambda)}{(1 + \lambda)K} & -\dfrac{m\lambda}{1 + \lambda} \\ \dfrac{K - \lambda}{K(1 + \lambda)} & 0 \end{pmatrix}
$$

and

$$
M_2 = \begin{pmatrix} \dfrac{\lambda(K - 1 - 2\lambda)}{(1 + \lambda)K} - 2a & -\dfrac{m\lambda}{1 + \lambda} \\ \dfrac{K - \lambda}{K(1 + \lambda)} & -2c \end{pmatrix}.
$$

Let λ_1, λ_2, λ_3, and λ_4 be the eigenvalues of (2.19), then we can assume that λ_1, λ_2 are the eigenvalues of M_1 and λ_3, λ_4 are the eigenvalues of M_2.

The local stability of $(\lambda, v_\lambda, \lambda, v_\lambda)$ is determined by the values of λ_1, λ_2, λ_3, and λ_4. If the real parts of all eigenvalues of J are negative, then the equilibrium $(\lambda, v_\lambda, \lambda, v_\lambda)$ is *stable*, otherwise it is *unstable*. When a single real eigenvalue crosses the boundary of stability as parameter changes, an *equilibrium bifurcation* will occur, and we can identify it if one of $\lambda_i = 0$; when a conjugated complex eigenvalue pair crosses the boundary of stability as parameter changes, a *Hopf bifurcation* (bifurcation of periodic orbits) will occur, and we can identify it if $\lambda_{1,2} = \pm bi$ or $\lambda_{3,4} = \pm bi$ for $b > 0$. From linear algebra, we will focus on the trace and determinant of M_1 and M_2 to find bifurcation points of the model.

Let $Tr(A)$ and $Det(A)$ denote the trace and determinant of a square matrix A. It is easy to show that

$$
Tr(M_1) = \frac{\lambda(K - 2\lambda - 1)}{(1 + \lambda)K}, \quad Det(M_1) = \frac{m\lambda}{1 + \lambda} \cdot \frac{K - \lambda}{K(1 + \lambda)},
$$

18

and

$$Tr(M_2) = \frac{\lambda(K - 2\lambda - 1)}{(1 + \lambda)K} - 2a - 2c = Tr(M_1) - 2(a + c),$$

$$Det(M_2) = \frac{m\lambda}{1 + \lambda} \cdot \frac{K - \lambda}{K(1 + \lambda)} - 2c\frac{\lambda(K - 2\lambda - 1)}{(1 + \lambda)K} + 4ac = Det(M_1) - 2cTr(M_1) + 4ac.$$

The matrix M_1 determines the local stability of (λ, v_λ) with respect to one-patch model (2.1). Recall from the analysis in Section 2.1 that, when $\frac{K - 1}{2} < \lambda < K$, $Tr(M_1) < 0$ and $Det(M_1) > 0$. Then it is easy to see that $Tr(M_2) < 0$ and $Det(M_2) > 0$ for $\frac{K - 1}{2} < \lambda < K$. Thus $(2\lambda, 2v_\lambda, 0, 0)$ is locally stable when $\frac{K - 1}{2} < \lambda < K$.

When $0 < \lambda < \frac{K - 1}{2}$, the signs of $Tr(M_2)$ and $Det(M_2)$ could change. Choosing λ as the bifurcation parameter, we want to investigate for which values of $a > 0$ and $c > 0$, there are bifurcation points.

2.4.1 Hopf bifurcations

Suppose that $\lambda = \lambda_H \in \left(0, \frac{K - 1}{2}\right)$ is a Hopf bifurcation point. With eigenvalues being $\pm bi$, it must be true that $Tr(M_2) = 0$ and $Det(M_2) > 0$. Thus we seek a and c that satisfies both conditions given below.

CONDITION H1 : $Tr(M_2) = 0$ at λ_H.

Define

$$h_1(\lambda) = \frac{\lambda(K - 2\lambda - 1)}{(1 + \lambda)K}.$$

After taking derivative of $h_1(\lambda)$ with respect to λ, we find that the function $h_1(\lambda)$ is increasing in $(0, \lambda_a)$ and it is decreasing in $(\lambda_a, (K - 1)/2)$, where $\lambda_a = 2\sqrt{2K - 2} - 1$ is the only critical point of $h_1(\lambda)$ in $\left(0, \frac{K - 1}{2}\right)$. Let $h_1(\lambda_a) = M^*$ which only depends on K. Then $\max_{\lambda \in [0, (K-1)/2]} Tr(M_2) = M^* - 2(a + c)$ is achieved at $\lambda = \lambda_a$.

- If $2(a + c) < M^*$, $Tr(M_2) < 0$ for all $0 < \lambda < \frac{K - 1}{2}$, and there will be no Hopf bifurcation points.

19

- If $2(a + c) > M^*$, then there are exactly two λ values so that $Tr(M_2) = 0$, with one in $(0, \lambda_a)$ and one in $(\lambda_a, (K-1)/2)$.

CONDITION H2: $Det(M_2) > 0$ at λ_H.

Notice that $Det(M_2)$ can also be written as

$$Det(M_2) = \frac{\lambda(K - 2\lambda - 1)}{(1 + \lambda)K} \left[\frac{m(K - \lambda)}{(1 + \lambda)(K - 2\lambda - 1)} - 2c \right] + 4ac$$

$$= c \cdot (h_1(\lambda) \left[m_c h_2(\lambda) - 2 \right] + 4a)$$

where

$$h_2(\lambda) = \frac{(K - \lambda)}{(1 + \lambda)(K - 2\lambda - 1)}, \quad \text{and} \quad m_c = \frac{m}{c}.$$

After taking the derivative of $h_2(\lambda)$ with respect to λ, we find that $h_2(\lambda)$ is positive and it has a positive minimum value M_* when $0 < \lambda < \dfrac{K - 1}{2}$. The minimum value M_* is either achieved at $\lambda_b = \dfrac{(\sqrt{2} - 1)K - 1}{\sqrt{2}}$ or at $\lambda = 0$. Hence if $m_c M_* > 2$ then $Det(M_2)$ is always positive, and the condition is automatically satisfied. We notice that $m_c M_* > 2$ is equivalent to

$$0 < c < \frac{mM_*}{2}.$$

In summary of the investigation of the above two conditions, if

$$2(a + c) > M^* \quad \text{and} \quad 0 < c < \frac{mM_*}{2}, \tag{2.20}$$

then there exist two Hopf bifurcation points λ_H^1 and λ_H^2. We remark that the condition for (a, c) is sufficient but not necessary for existence of Hopf bifurcation points.

2.4.2 Equilibrium Bifurcations

With one of the eigenvalues of M_2 being 0, the conditions for an equilibrium bifurcation to occur require that $Tr(M_2) \neq 0$ and $Det(M_2) = 0$. Thus, we look for a and c that produce λ-values λ_E satisfying both conditions.

CONDITION E1 : $Tr(M_2) \neq 0$ at λ_E.

We can deduce from previous discussions on Hopf bifurcation that for all $a > 0$ and $c > 0$, there are at most two λ-values so that $Tr(M_2) = 0$. Hence only for exceptional values of a and c, $Tr(M_2) = 0$ and $Det(M_2) = 0$ occur at the same time.

CONDITION E2: $Det(M_2) = 0$ at λ_E.

Notice that

$$h_3(\lambda) = K(1+\lambda)^2 \cdot Det(M_2) = m\lambda(K-\lambda) - 2c\lambda(1+\lambda)(K-2\lambda-1) + 4Kac(1+\lambda)^2,$$

is a cubic polynomial, and $Det(M_2) = 0$ is equivalent to $h_3(\lambda) = 0$. Hence there are at most three λ-values which make $Det(M_2) = 0$. In fact, $h_3(0) = 0$ and, for any $c > 0$, $\lim_{\lambda \to -\infty} h_3(\lambda) = -\infty$, so $h_3(\lambda) = 0$ has at least one negative root from intermediate value theorem in calculus. Therefore there are at most two positive λ-values which make $Det(M_2) = 0$. As $h_3(0) = 0$ and $h_3((K-1)/2) > 0$, then for most parameter values, we should have two or zero positive λ-values in $(0, (K-1)/2)$ such $Det(M_2) = 0$.

To guarantee that there exist λ_E such that $Det(M_2) = 0$, one can make m and a smaller (but keep the c value constant) so that the negative term in $h_3(\lambda)$ can dominate the positive terms. To be more precise, we only need $\min_{\lambda \in [0, (K-1)/2]} h_3(\lambda) < 0$. We observe that for $\lambda \in [0, (K-1)/2]$,

$$\lambda(K - \lambda) \leq \frac{K^2}{4}, \quad \text{and} \quad 4Kac(1+\lambda)^2 \leq Kac(K+1)^2.$$

Hence

$$h_3(\lambda) \leq \frac{mK^2}{4} + Kac(K+1)^2 - 2c\lambda(1+\lambda)(K-2\lambda-1),$$

and

$$
\begin{aligned}
\min_{\lambda \in [0, (K-1)/2]} h_3(\lambda) &\leq h_3\left(\frac{K-1}{4}\right) \\
&\leq \frac{mK^2}{4} + Kac(K+1)^2 - \frac{c(K-1)(K+1)(K+3)}{16} \\
&\leq \frac{mK^2}{4} + Kac(K+1)^2 - \frac{c(K-1)(K+1)K}{16} \\
&\leq 0,
\end{aligned}
$$

21

if we make

$$c > \frac{8m}{K} \quad \text{and} \quad 0 < a < \frac{1}{32}. \tag{2.21}$$

In summary of the investigation of the above two conditions, for $a > 0$ and $c > 0$ satisfying (2.21) (but may exclude finite many exceptional values), there exist two equilibrium bifurcation points λ_E^- and λ_E^+ that lie in $(0, \frac{K-1}{2})$.

2.4.3 Numerical examples and numerical bifurcation diagrams

We have identified conditions on diffusion rates a and c so that Hopf bifurcations and equilibrium bifurcations can occur for certain $\lambda \in \left(0, \frac{K-1}{2}\right)$. In general for most given values of (a, c), (2.15) and (2.16) can have one, tow or three Hopf bifurcation points, and zero or two equilibrium bifurcation points for $\lambda \in (0, K)$.

In this subsection, we use numerical examples to show all these numbers are possible, and for each case we use `MatCont`, a software package based on `Matlab`, to produce a corresponding numerical bifurcation diagram. In each of Fig. 2.2, 2.3 and 2.4, the left panel shows the graphs of $Tr(M_2)$ and $Det(M_2)$ as functions of parameter λ. From the discussions presented above, a Hopf bifurcation point $\lambda = \lambda_H$ satisfies $Tr(M_2) = 0$ and $Det(M_2) > 0$, while an equilibrium bifurcation point $\lambda = \lambda_E$ satisfies $Tr(M_2) \neq 0$ and $Det(M_2) = 0$.

In each bifurcation diagram on the right panel of Figure 2.2, 2.3 and 2.4, the curve emerged from $(e, u) = (0, 0)$ and ended at $(e, u) = (e_{max}, 5)$ (in all graphs, $K = 5$) is the curve of equilibria $(e, u, v, w, x) = (e, \lambda, v_\lambda, \lambda, v_\lambda)$. The upper bound $(e, u) = (e_{max}, 5)$ is where it meets the line of trivial solution $(e, u, v, w, x) = (e, K, 0, K, 0) = (e, 5, 0, 5, 0)$. In each bifurcation diagram, the first bifurcation point on the left of e_{max} is the Hopf bifurcation for the symmetric periodic orbits, which is where $Tr(M_1) = 0$ ($Tr(M_1) > 0$ always holds). From results in Section 2.1, this curve of periodic orbits can be extended to all $e > 0$. This part of bifurcation diagram is same as the one for one-patch model (2.1).
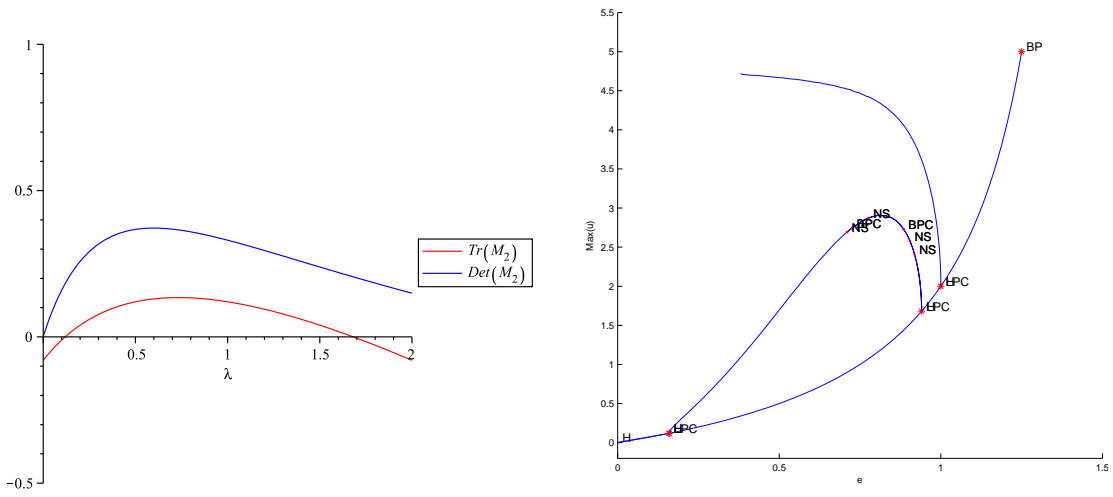
(a) Graphs of $Tr(M_2)$ and $Det(M_2)$ (b) Bifurcation diagram

Figure 2.2: Two Hopf bifurcations and no equilibrium bifurcation. with $K = 5$, $m = 1.5$, $a = 0.03$ and $c = 0.01$. In (a), the horizontal axis is λ, and the vertical axis is the values of $Tr(M_2)$ and $Det(M_2)$; in (b), the horizontal axis (bifurcation parameter) is e, and the vertical axis is u for equilibria and the maximum of u for periodic orbits.

For $0 < \lambda < \dfrac{K-1}{2}$, the bifurcation structure of three graphs in Figure 2.2, 2.3 and 2.4 are dramatically different. In Figure 2.2, there are two additional Hopf bifurcation points where asymmetric periodic orbits bifurcate from the symmetric equilibria $(\lambda, v_\lambda, \lambda, v_\lambda)$. The branch of asymmetric periodic orbits appears to be a loop which joins two Hopf bifurcation points. On the branch of asymmetric periodic orbits, there are four Neimark-Sacker bifurcation points (NS) and two branching points of periodic orbits (BPC). Investigating these secondary bifurcations is beyond the scope of this thesis, but the presence of these additional bifurcation points shows that the 2-patch model has much richer structure than the 1-patch one.

In Figure 2.3, there are two additional equilibrium bifurcation points where asymmetric equilibria bifurcate from the curve of symmetric equilibria $(\lambda, v_\lambda, \lambda, v_\lambda)$. Again the branch of asymmetric equilibria is a loop. The curves above and below the primary curve shows
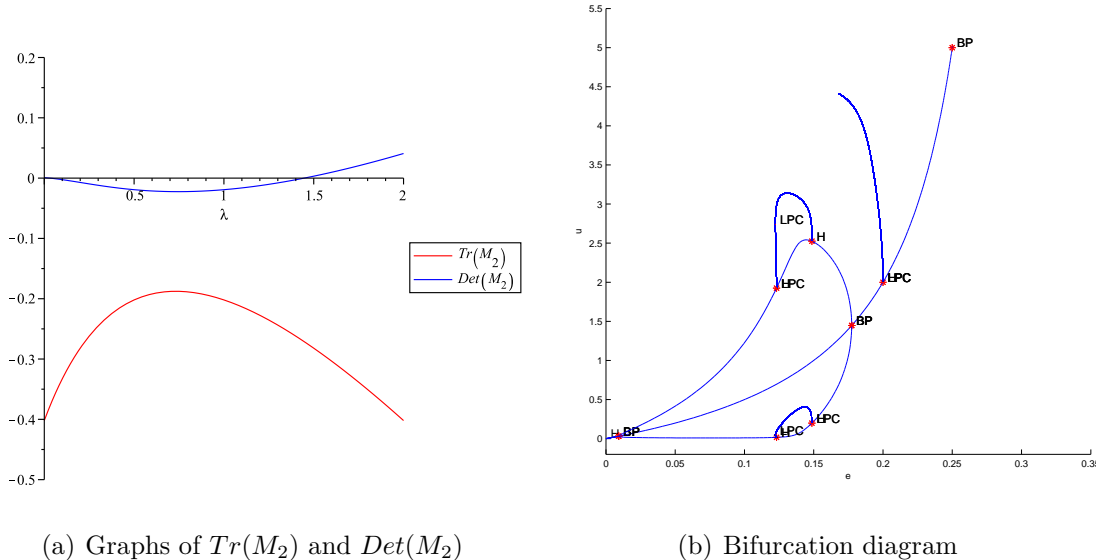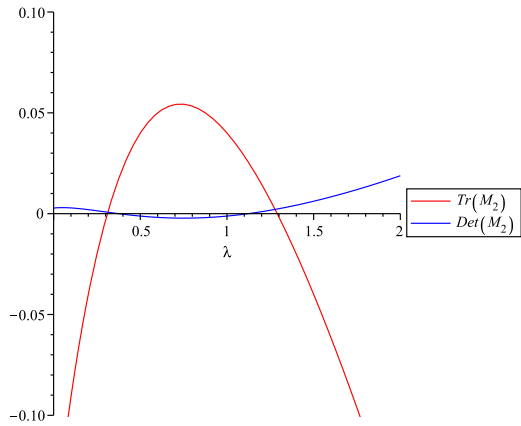
23

(a) Graphs of $Tr(M_2)$ and $Det(M_2)$ (b) Bifurcation diagram

Figure 2.3: Two equilibrium bifurcations and no Hopf bifurcation. Here $K = 5$, $m = 0.3$, $a = 0.001$ and $c = 0.2$. In (a), the horizontal axis is λ, and the vertical axis is the values of $Tr(M_2)$ and $Det(M_2)$; In (b), the horizontal axis (bifurcation parameter) is e, and the vertical axis is u for equilibria and the maximum of u for periodic orbits.

two additional equilibria between the two bifurcation points, which are symmetric if we switch (u, v) and (w, x). The two equilibrium bifurcations are both pitchfork bifurcations. For that range of e (or λ), the system has five equilibria. It is possible to find an analytic form of these equilibria, as the equations are polynomials. One can show that the system has at most nine equilibria from the fundamental theorem of algebra. Indeed Jansen [16] found the exact form of nine equilibria when $a = 0$ (immobile preys). We also note that there are two secondary Hopf bifurcation points on the curve of asymmetric equilibria, and asymmetric periodic orbits bifurcate from there, which shows the system can have three periodic orbits for some e.

Finally in Figure 2.4, there are two additional Hopf bifurcation points and two additional equilibrium bifurcation points. The loop of asymmetric equilibria contains two pairs of Hopf bifurcation points, and the curve of periodic orbits also possesses more

(a) Graphs of $Tr(M_2)$ and $Det(M_2)$
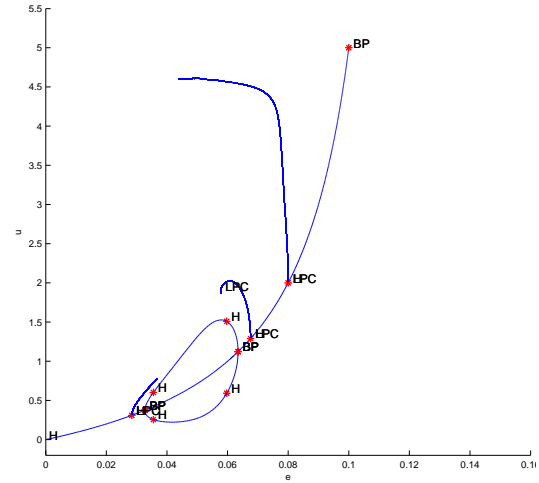
(b) Bifurcation diagram

Figure 2.4: Two Hopf Bifurcations and Equilibrium Bifurcations. Here $K = 5$, $m = 0.12$, $a = 0.01$ and $c = 0.07$. In (a), the horizontal axis is λ, and the vertical axis is the values of $Tr(M_2)$ and $Det(M_2)$; in (b), the horizontal axis (bifurcation parameter) is e, and the vertical axis is u for equilibria and the maximum of u for periodic orbits.

bifurcation points, which needs further investigation.

Overall these bifurcation diagrams show that the 2-patch model could have many more equilibria and periodic orbits even when the two patches are identical. The number of such asymmetric equilibria and periodic orbits sensitively depends on the diffusion rates a and c, as well as m (the strength of the predator-prey interaction).

Chapter 3

Numerical Simulation of the Non-Symmetric Model

3.1 Non-Symmetric Model

In order to observe the dynamic behavior of the model in a more realistic context, we revise our symmetrical model by adding spatial heterogeneity to it. Specifically, for equation (2.8), we assume same carrying capacity, K, has the same saturation value of the functional response, m. However, we make the death rates of predators different from one to each other ($e_1 \neq e_2$). One possible explanation of this modification could be the environment in one patch is more suitable for the predator to live. Hence the equation to consider in this chapter is

$$
\begin{cases}
u' = u\left(1 - \dfrac{u}{K}\right) - \dfrac{muv}{1+u} + a(w-u), \\[2mm]
v' = \dfrac{muv}{1+u} - e_1 v + c(x-v), \\[2mm]
w' = w\left(1 - \dfrac{w}{K}\right) - \dfrac{mwx}{1+w} - a(w-u), \\[2mm]
x' = \dfrac{mwx}{1+w} - e_2 x - c(x-v).
\end{cases}
\tag{3.1}
$$

From the conclusions of Section 2.1 on single-patch predator-prey, we know that the local system has its Hopf bifurcation at $\lambda = \dfrac{K-1}{2}$. When $0 < \lambda < \dfrac{K-1}{2}$, the local system has a limit cycle; when $\dfrac{K-1}{2} < \lambda < K$, the local system has a stable equilibrium (λ, v_λ); when $K < \lambda$. the local system has a stable equilibrium $(K, 0)$. In this asymmetric two-patch model, different predator death rates (often referred as an intrinsic environment heterogeneity factor) give rise to different values of λ_i, the respective steady states and limit cycles of each patch without migration. In this chapter, we are interested in the effect of migration on the metapopulation of two patches; thus we simulated the model with different sets of parameters.

3.2   Numerical Simulations

Jensen [16, 17] argued that weak coupling can reduce the chance of extinctions and can thus be a possible solution to the Paradox of Enrichment. We confirmed this statement when we coupled two oscillators through migration.

In Figure 3.1(a), patch-1 exhibits limit cycles where prey population is 0 for a long period, while patch-2 has much shorter limit cycles where prey extinction is not a threat. When we couple these two patches together through prey migration rate 0.1 and predator migration rate 0.2, the coupled population on the whole now has shorter limit cycle and prey population in patch-1 experience a much shorter period of zero prey population. In addition, we can identify a degree of synchronization since the prey populations in the two patches reach population highs and lows at the same time. The same applies to the predator population.

When the migration rates are larger, this synchronization becomes more obvious. In Figure 3.1:(b), migration rates are higher than Figure 3.1:(a), and a more obvious degree of synchronization can be identified. Both of the prey and predator populations in two patches have almost the exact same periodic cycle after coupling. This also leads to

another conclusion drew from these two figures. Larger the migration rates are, the more synchronized the system is. This also makes sense intuitively because more isolated patches tend to preserve their local population without coupling, and when the migration becomes very large, the two-patch system can be interpreted as one system with almost no boundaries.

We also found that when an oscillator is coupled with a patch with constant equilibrium, the population of the coupled system will converge and eventually reach a constant equilibrium. Figure 3.2 shows examples of this situation. In these figures, patch-1 represents a local patch with steady state and patch-2 is a oscillator. The meta-population of the coupled system shows periodic behavior at first and eventually converges to constant equilibrium. This is very encouraging evidence because it is additional support for the argument that regulation of ecological systems through migration is useful for the persistence of species. Again, by comparing Figure 3.2:(a) and Figure 3.2:(b), we found that greater migration rates give rise to shorter adjusting time for the coupled system to converge to steady equilibria.

Coupling two identical oscillating patches may lead to chaos in the system. Jensen's simulations in [16] with certain parameters generated a quasi-periodic solution and a chaotic solution. Our simulation yielded similar results.

Knowing the range of parameters for specific solutions of each local patch, we summarize the global population dynamics of the coupled system in Table 3.1.

patch 1 \ patch 2	predator extinction	coexistence	oscillation
predator extinction	predator extinction	predator extinction	coexistence
coexistence	predator extinction	coexistence	oscillation
oscillation	coexistence	oscillation	oscillation

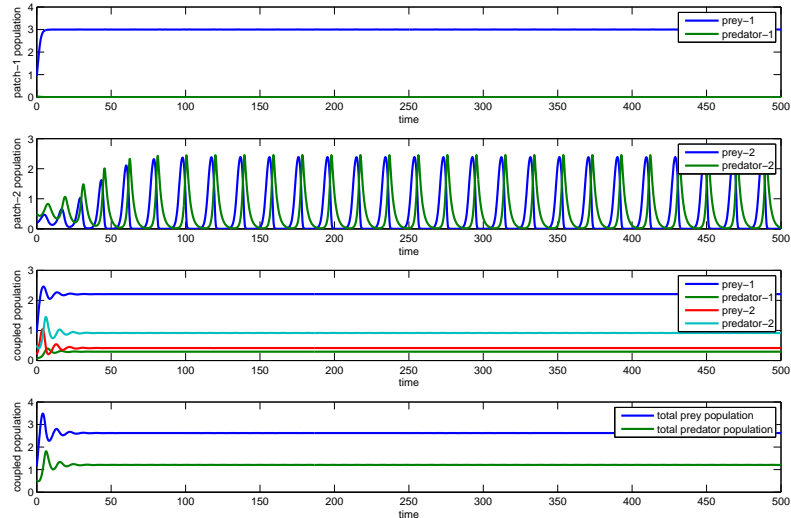Table 3.1: Summary of dynamics of two-patch predator-prey model
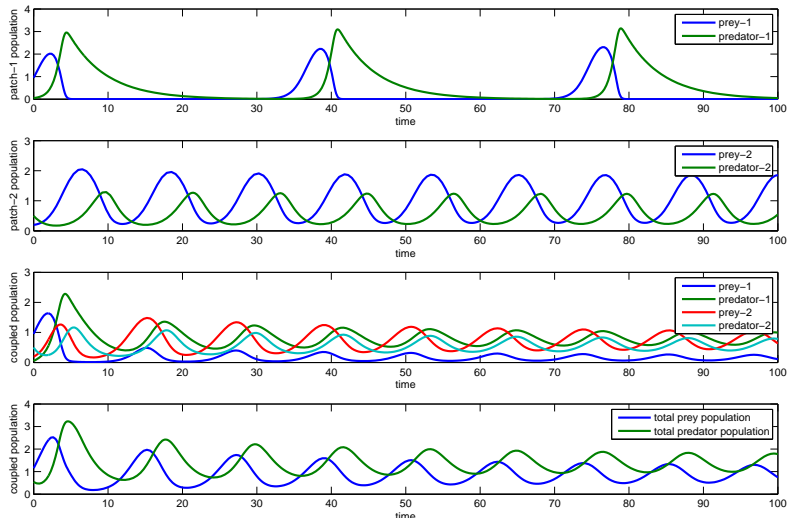
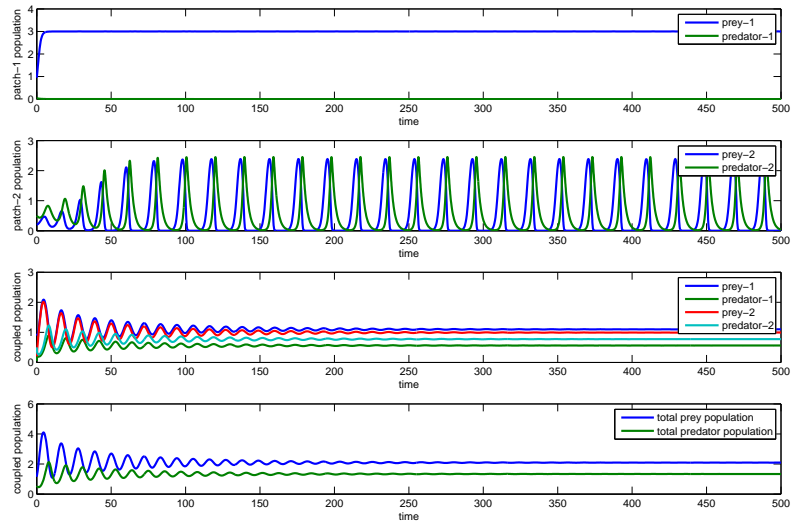(a) Diffusion rates: $a = 0.1$; $c = 0.2$.
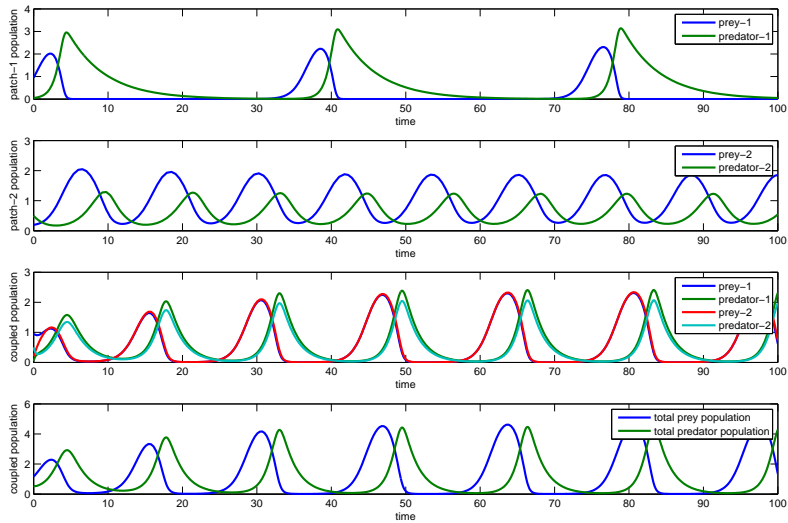
(b) Diffusion rates: $a = 1$; $c = 2$.

Figure 3.1: Oscillating patches coupled by diffusion rates. For both graphs, $x_0 = [0.95; 0.05; 0.2; 0.5]$; $k = 3$; $m = 2$; $e_1 = 0.2$; $e_2 = 0.9$.
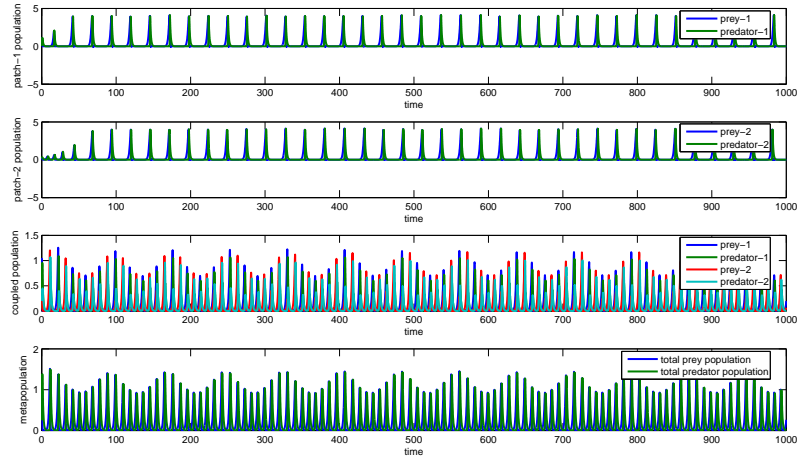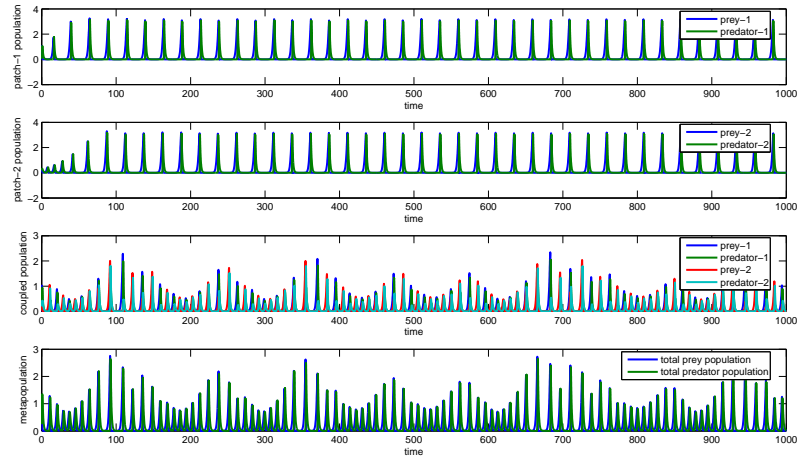
(a) Diffusion rates: $a = 0.1$; $c = 0.2$.

(b) Diffusion rates: $a = 1$; $c = 2$.

Figure 3.2: Oscillating and coexisting patches coupled by diffusion rates. For both graphs, $x_0 = [0.95; 0.05; 0.2; 0.5]$; $k = 3$; $m = 2$; $e_1 = 1.8$; $e_2 = 0.45$

(a) Quasi periodic solution: $k = 7$; $a = 0$; $c = 0.7$.

(b) Chaotic solution: $k = 5$; $a = 0$; $c = 0.6$.

Figure 3.3: Identical Oscillating Patches Coupling Yield Chaos. For both graphs, $x_0 = [0.95; 0.05; 0.2; 0.5]$; $m = 9.96$; $e_1 = 1$; $e_2 = 1$.

Chapter 4

Conclusions

This paper investigated the population dynamics of a coupled predator-prey model. Our model is based on the Rosenzweig–MacArthur predator-prey model with Holling Type II functional response. We conducted mathematical and numerical analysis on the symmetric two-patch models.

Based on the existing knowledge of the one patch model, we proved the steady states $(K, 0, K, 0)$ and $(\lambda, v_\lambda, \lambda, v_\lambda)$ are globally stable using Lyapunov functional. We then conducted local stability analysis after tweaking the model using population sums and differences. By studying the Jacobian matrix, we were able to identify different cases of bifurcation results and some necessary conditions for each case. Using computing software `Maple` and `Matcont`, this paper provided specific examples. This paper approached the non-symmetric system only through numerical simulations due to the difficulty of conducting mathematical analysis generated by increased number of parameters. Results from numerical simulations support recent supposition to use coupling as a possible solution to the Paradox of Enrichment. Different degrees of coupling in some systems with certain parameters show different degrees of synchronization, and usually decrease the chance of population extinction to a certain extent.

This study can also be compared with results in a recent paper [32], where a Rosenzweig–

MacArthur predator-prey partial differential equation model is considered. In [32], the bifurcation of periodic orbits and equilibria were also showed with the spatial domain being an interval. Our results here show that even a discrete spatial model can produce such complexity of bifurcation structure. However we have also observed from our studies, that even for the simple two patch model with four ordinary differential equations, a complete classification of the dynamics is still out of reach.

4.1 Acknowledgements

Bibliography

[1] Berryman, A. A., The origins and evolution of predator-prey theory. *Ecology* **73** (1992), no.5, 1530–1535.

[2] Cheng, K. S., Uniqueness of a limit cycle for a predator-prey system. *SIAM J. Math. Anal.* **12** (1981), 541–548.

[3] Commins, H. N.; Hassell, M. P., Persistence of multispecies host-psrastoid interactions in spatially distributed models with local dispersal. *J. Theo. Biol.* **183** (1996), 19–28.

[4] de Mottoni, P.; Rothe, F., Convergence to homogeneous equilibrium state for generalized Volterra-Lotka systems with diffusion. *SIAM J. Appl. Math.* **37** (1979), no. 3, 648–663.

[5] Goldwyn, E. E.; Hastings, A., Small heterogeneity has large effects on synchronization of ecological oscillators. *Bulletin of Mathematical Biology* **71** (2009), 130–144.

[6] Goldwyn, E. E.; Hastings, A., When can dispersal synchronize populations? *Theo. Popu. Biol.* **73** (2008), 395–402.

[7] Gotelli, N. J., A Primer of Ecology. 4th edition. Sinauer Associates, Inc., Sunderland, MA. 2008.

[8] Holland, M. D.; Hastings, A., Strong effect of dispersal network structure on ecological dynamics. *Nature* **456** (2008), 792–795.

[9] Holling, C. S., The components of predation as revealed by a study of small mammal predation of the European Pine Sawfly. *Canadian Entomologist.* **91** (1959), 293–320.

[10] Holt, R. D., Spatial Heterogeneity, indirect interactions, ans the coexistence of prey species. *The American Naturalist* **124** (1984), no. 3, 377–406.

[11] Horsthemke, W.; Moore, P. K., Turing instability in inhomogeneous arrays of diffusively coupled reactors. *J. Phys. Chem. A* **108** (2004), no. 12, 2225–2231.

[12] Hsu, S. B., On global stability of a predator-prey system. *Math. Biosci.* **39** (1978), no. 1–2, 1–10.

[13] Hsu, S. B., A survey of constructing Lyapunov functions for mathematical models in population biology. *Taiwanese Journal of Mathematics* **9** (2005), no. 2, 151–173.

[14] Hsu, S. B.; Shi, J. P., Relaxation oscillator profile of limit cycle in predator-prey system. *Disc. Cont. Dyna. Syst.-B* **11** (2009) no. 4, 893–911.

[15] Kuang, Y.; Freedman, H. I., Uniqueness of limit cycles in Gause-type models of predator-prey systems. *Math. Biosci.* **88** (1988), 67–84.

[16] Jansen, V. A. A., Regulation of predator-prey systems through spatial interactions: a possible solution to the paradox of enrichment. *Oikos* **74** (1995), no. 3, 384–390.

[17] Jansen, V. A. A., The dynamics of two diffusively coupled predator-prey populations. *Theoretical Population Biology* **59** (2001), 119–131.

[18] Lotka, A. J., Analytical Note on Certain Rhythmic Relations in Organic Systems. *Proc. Natl. Acad. Sci.* **6** (1920), no. 7, 410–415.

[19] Lotka, A. J., Elements of Physical Biology. Williams and Wilkins, Baltimore, Maryland, 1925.

[20] Lengyel, I.; Epstein, I. R., Diffudion-induced instability in chemically reacting systems: Steady-state multiplicity, oscillation and chaos. *CHAOS* **1** (1991), no.1, 69–75.

[21] Leslie, P. H., Some furthur notes on the use of matrices in population mathematics. *Biometrica* **35** (1948), 213–245.

[22] May, R. M., Limit cycles in predator-prey communities. *Science* **177**, (1972), 900–902.

[23] Maynard Smith, J. Models in Ecology. Cambridge University Press. 1974.

[24] Murdoch, W. M.; Briggs, C. J.; Nisbet, R. M., Consumer-Resource Dynamics. Princeton University Press, Princeton, 2003.

[25] Pearl, R., The Biology of Population Growth. Alfred A. Knopf, New York, 1925.

[26] Rosenzweig, M. L., Paradox of enrichment: destablization of exploitation ecosystems in ecological time. *Science* **171** (1971), no. 3969, 385–387.

[27] Real, L., The kenetics of functional response. *American Naturalist* **111** (1977), 289–300.

[28] Rosenzweig, M. L.; MacArthur, R., Graphical representation and stability conditions of predator-prey interactions. *Amer. Natur.* **97** (1963), 209–223.

[29] Rovinsky, A.; Menzinger, M., Interaction of Turing and Hopf bifurcation in chemical system. *Phys. Rev. Lett.* **46** (1992), no.10, 6315–6322.

[30] Solomon, M. E., The Natiral control of animal population. *Journal of Animal Ecology* **18** (1949), 1–35.

[31] Volterra, V., Fluctuations in the Abundance of a Species Considered Mathematically. *Nature* **118** (1926), 558–560.

[32] Yi, F. Q.; Wei, J. J.; Shi, J. P., Bifurcation and spatiotemporal patterns in a homogeneous diffusive predator-prey system. *J. Differential Equations* **246** (2009), no. 5, 1944–1977.